Molecular Basis of Isoform-specific μ-Conotoxin Block of Cardiac, Skeletal Muscle, and Brain Na$^+$ Channels*

Ronald A. Li‡§, Irene L. Ennis‡¶‖, Tian Xue‡, Hai M. Nguyen, Gordon F. Tomaselli‡, Alan L. Goldin**, and Eduardo Marbán‡ ‡‡**

*From the ‡Institute of Molecular Cardiobiology, The Johns Hopkins University School of Medicine, Baltimore, Maryland 21205 and the **Department of Microbiology and Molecular Genetics, University of California, Irvine, California 92697*

μ-Conotoxins (μ-CTXs) block skeletal muscle Na$^+$ channels with an affinity 1–2 orders of magnitude higher than cardiac and brain Na$^+$ channels. Although a number of conserved pore residues are recognized as critical determinants of μ-CTX block, the molecular basis of isoform-specific toxin sensitivity remains unresolved. Sequence comparison of the domain II (DII) S5-S6 loops of rat skeletal muscle (μ1, Na$_v$1.4), human heart (hh1, Na$_v$1.5), and rat brain (rb1, Na$_v$1.1) Na$^+$ channels reveals substantial divergence in their N-terminal S5-P linkers even though the P-S6 and C-terminal P segments are almost identical. We used Na$_v$1.4 as the backbone and systematically converted these DII S5-P isoform variants to the corresponding residues in Na$_v$1.1 and Na$_v$1.5. The Na$_v$1.4→Na$_v$1.5 variant substitutions V724R, C725S, A728S, D730S, and C731S (Na$_v$1.4 numbering) reduced block of Na$_v$1.4 by 4-, 86-, 12-, 185-, and 55-fold respectively, rendering the skeletal muscle isoform more "cardiac-like." Conversely, an Na$_v$1.5→Na$_v$1.4 chimeric construct in which the Na$_v$1.4 DII S5-P linker replaces the analogous segment in Na$_v$1.5 showed enhanced μ-CTX block. However, these variant determinants are conserved between Na$_v$1.1 and Na$_v$1.4 and thus cannot explain their different sensitivities to μ-CTX. Comparison of their sequences reveals two variants at Na$_v$1.4 positions 729 and 732: Ser and Asn in Na$_v$1.4 compared with Thr and Lys in Na$_v$1.1, respectively. The double mutation S729T/N732K rendered Na$_v$1.4 more "brain-like" (30-fold ↓ in block), and the converse mutation T925S/K928N in Na$_v$1.1 reproduced the high affinity blocking phenotype of Na$_v$1.4. We conclude that the DII S5-P linker, although lying outside the conventional ion-conducting pore, plays a prominent role in μ-CTX binding, thus shaping isoform-specific toxin sensitivity.

μ-Conotoxins (μ-CTXs)[1] are guanidinium toxins that are produced by the sea snail *Conus geographus* (1–5) and block

Na$^+$ channels by physical occlusion of the pore (2, 6–10). Although chemically dissimilar to the pufferfish-derived tetrodotoxin (TTX) and the red tide saxitoxin (STX), μ-CTXs show biological actions similar to those of TTX and STX. Like TTX and STX, μ-CTXs block Na$^+$ channels from different tissues with vastly different affinities. μ-CTXs preferentially block skeletal muscle and eel Na$^+$ channels with affinities 2 orders of magnitude higher than for block of the cardiac and brain counterparts. In contrast, brain and skeletal muscle channels are 3 orders of magnitude more sensitive to TTX/STX than are heart channels (11–15). Although the key determinant for isoform-specific TTX and STX block has been identified (tyrosine and phenylalanine in the domain I (DI) P loop of the TTX/STX-sensitive skeletal muscle and brain isoforms, respectively, but cysteine at the homologous position in the toxin-resistant cardiac subtype (16–18)), previous attempts to study isoform-specific μ-CTX block have been largely unsuccessful because its determinants are more widespread and have a much larger footprint in the channel pore than the compact TTX and STX (8–10, 14, 15, 19–23).

The S5-S6 linkers that form the outer pore vestibule and the selectivity filter are divided into three regions: S5-P, P loop (whose descending and ascending regions are referred to as SS1 and SS2, respectively), and P-S6 (see Fig. 1A) (11). Even though homologous regions are found in all four S5-P linkers of different Na$^+$ channel isoforms, those of domains I–III display substantial divergence. DIII and DIV have small variable regions distal to the highly conserved P loops. To date, all critical determinants for μ-CTX block identified in the conventional aqueous pore formed by the P loop SS2s (11) and the P-S6 linkers (10, 24) are residues that are invariant in cardiac, skeletal muscle, and brain channels (8–10, 23). Therefore, they cannot explain the vast differences in isoform-specific μ-CTX sensitivity. Chimeric studies have demonstrated that DI and especially DII are more critical determinants of isoform-specific μ-CTX affinity than are DIII and DIV (the rat skeletal muscle (Na$_v$1.4) Na$^+$ channels carrying the entire DI or DII from the human heart (Na$_v$1.5) isoform were ~20- and >200-fold less sensitive, respectively, than wild-type (WT) Na$_v$1.4 (14, 15); however, the detailed molecular basis remains unresolved. Sequence inspection of the DII S5-S6 loops of the toxin-sensitive Na$_v$1.4 and the toxin-resistant rat brain (Na$_v$1.1) and Na$_v$1.5 Na$^+$ channels reveals substantial divergence in their S5-P linkers, although the C-terminal portions (*i.e.* P and P-S6) that form the conventional ion-conducting pore are almost identical (for sequence comparisons, see Figs. 1B and 4A). Because many of the known toxin determinants are clustered in the DII pore region (8–10, 23), the divergence of the adjacent DII S5-P

[1] The abbreviations used are: μ-CTX, μ-conotoxin(s); B-to-M, brain-to-muscle; DI, DII, DIII, DIV, domains I, II, III, and IV, respectively; H-to-M, heart-to-muscle; STX, saxitoxin; TTX, tetrodotoxin; WT, wild-type.
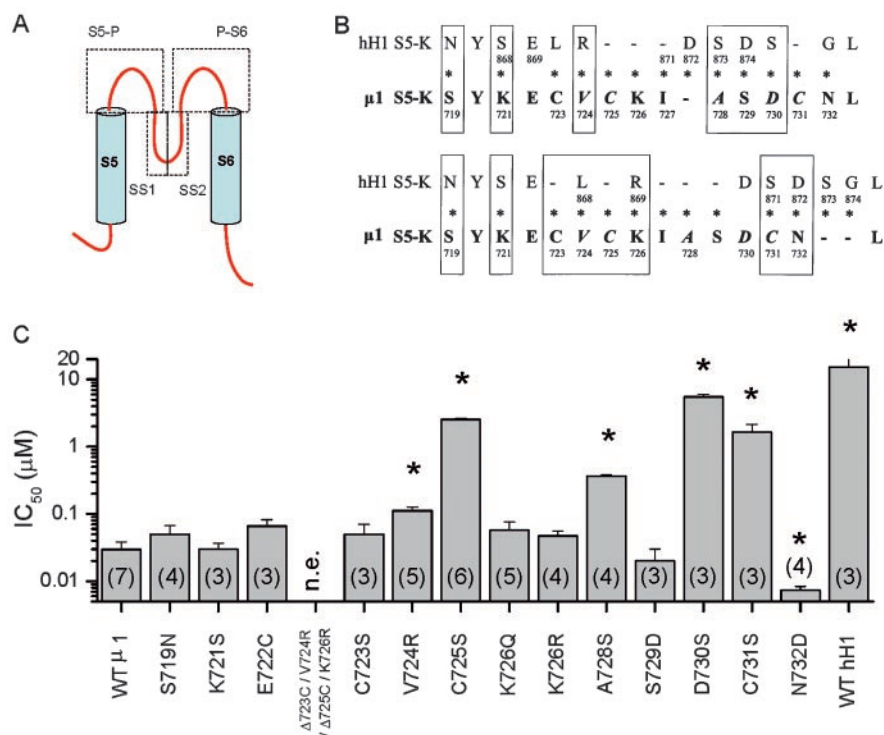
FIG. 1. **Effects of DII S5-P isoform variants between Na$_v$1.4 and Na$_v$1.5 on μ-CTX block.** *A*, schematic diagram showing the S5 and S6 transmembrane segments and the reentrant S5-S6 linker. The S5-S6 linker consists of the S5-P, P loop (*i.e.* SS1 and SS2), and P-S6 linker. *B*, comparison of the primary sequences of the DII S5-P linker of human cardiac (Na$_v$1.5) and rat skeletal muscle (Na$_v$1.4, *bold*) Na$^+$ channels. The S5-P linker is N-terminal to the conventional aqueous pore formed by the P loop and the P-S6 linker and displays substantial divergence among different isoforms of Na$^+$ channels. Sequence alignment of the two isoforms is ambiguous because the DII S5-P linkers are different lengths. Thus, there are many different possible alignments of this region of the channels, two of which are shown. *Asterisks* indicate isoform-specific amino acid variants within a given alignment. The mutated Na$_v$1.4 residues are *boxed*. Those that reduced toxin sensitivity are shown in *italics*. *C*, *bar graphs* summarizing the half-blocking concentrations (IC$_{50}$) of WT and DII S5-P mutant Na$_v$1.4 channels for block by μ-CTX GIIIB. The isoform variants C723S, V724R, A728S, D730S, and C731S significantly reduced block by μ-CTX. Data shown are the mean ± S.E. *Numbers* in *parentheses* represent the number of determinations for each of the individual *bars*, with *asterisks* indicating statistical differences ($p < 0.05$). *n.e.*, not expressed.

linker motivated us to test whether the differences therein might underlie isoform-specific μ-CTX block. To test this hypothesis, we systematically converted the isoform-specific variants in Na$_v$1.4 to those in Na$_v$1.1 and Na$_v$1.5 and vice versa and then assayed their effects on μ-CTX sensitivity. We identified DII S5-P variants that prominently determine isoform-specific μ-CTX block. The molecular basis of isoform-specific μ-CTX block is discussed in the context of structural implications of the sodium channel pore. A preliminary report has appeared (25).

EXPERIMENTAL PROCEDURES

Site-directed Mutagenesis and Heterologous Expression—The gene encoding Na$_v$1.4 or Na$_v$1.5 sodium channels was cloned into the pGFP-IRES vector with an internal ribosomal entry site separating it from the green fluorescent protein (GFP) reporter gene (26); that of Na$_v$1.1 was cloned into pLCT1 (27). Mutagenesis was performed using PCR with overlapping mutagenic primers. The presence of the desired mutation(s) was confirmed by DNA sequencing. Na$_v$1.4 and Na$_v$1.5 channels were transfected into tsA-201 cells using LipofectAMINE Plus (Invitrogen) according to the manufacturer's protocol. Briefly, plasmid DNA encoding the WT or mutant α subunit (1 μg/60-mm dish) was added to the cells with LipofectAMINE, followed by incubation at 37 °C in a humidified atmosphere of 95% O$_2$, 5% CO$_2$ for 48–72 h before electrical recordings. For Na$_v$1.1 channels, cRNA was transcribed from *Not*I-linearized DNA using T7 RNA polymerase (Promega, Madison, WI) and coinjected with the rat brain β1 subunit into *Xenopus* oocytes for heterologous expression as described (9, 28).

Electrophysiology and Data Analysis—Electrophysiological recordings were performed at room temperature using the whole cell patch clamp technique (29) for tsA-201 cells and two-electrode voltage clamp recordings for oocytes. Transfected tsA-201cells were identified by epifluorescence microscopy from the coexpressed green fluorescent protein.

Patch pipette electrodes had final tip resistances of 1–3 megohms; the internal recording solution contained (in mM): 35 NaCl, 105 CsF, 1 MgCl$_2$, 10 HEPES, 1 EGTA, pH adjusted to 7.2 with CsOH. For oocyte recordings, the pipette contained 3 M KCl and had final tip resistances of 2–4 megohms. All electrical recordings were performed in a bath solution containing (in mM): 140 NaCl, 5 KCl, 2 CaCl$_2$, 1 MgCl$_2$, 10 HEPES, 10 glucose, pH adjusted to 7.4 with NaOH. Designated amounts of μ-CTX were added to the bath when required.

Toxin was superfused continuously during the experiment at ~10 ml/min (bath volume was 150 μl). Raw current records were analyzed using custom written software. Half-blocking concentrations (IC$_{50}$) for μ-CTX were determined by fitting the dose-response data to the binding isotherm,

$$I/I_O = 1/\{1 + ([\text{toxin}]/\text{IC}_{50})\} \qquad (\text{Eq. 1})$$

where IC$_{50}$ is the half-blocking concentration, [toxin] is the toxin concentration, and I_0 and I are the peak currents measured from a step depolarization to -10 mV from a holding potential of -100 mV before and after application of the blocker, respectively. Concentrations of 30 and/or 100 nM μ-CTX were initially used to screen mutants for changes in sensitivity. Depending on the sensitivity, concentrations used for subsequent experiments were chosen to bracket the IC$_{50}$ of a particular mutant (*e.g.* 1 and 3 μM for C731S).

All data reported are the mean ± S.E. Statistical significance was determined using a paired Student's *t* test at the 5% level.

RESULTS

Amino Acid Differences in the Conventional Pore Are Not Responsible for Isoform-specific μ-CTX GIIIB Sensitivity—We first compared the μ-CTX GIIIB sensitivity of WT Na$_v$1.4 and Na$_v$1.5 Na$^+$ channels (Fig. 1*B*). Consistent with previous studies (12, 14, 15, 30), Na$_v$1.4 (IC$_{50}$ = 29.7 ± 8.6 nM; *n* = 7) was

substantially more susceptible to μ-CTX block than $Na_v1.5$ (IC_{50} = 15.3 ± 7.7 μM; n = 3; p < 0.01). This vast isoform-specific difference in toxin block prompted us to investigate the underlying molecular basis. Even though the P loops of $Na_v1.4$ and $Na_v1.5$ Na^+ channels are highly conserved, a number of differences do exist. One such difference is the residue at position 401 in DI ($Na_v1.4$ numbering throughout this manuscript unless otherwise specified). Although replacing Tyr[401] with a cysteine could largely explain the isoform-specific differences in TTX and STX block observed with $Na_v1.4$ and $Na_v1.5$ channels (16, 18), this mutation had little effect on μ-CTX block (9, 14). Despite the lack of a significant role for this pore residue, it is still conceivable that other differences in the pore, especially those involving a charge difference, may be responsible for isoform-specific μ-CTX block. Charge-variant residues in the pore include DIII Glu[1251], DIII Lys[1252], and DIV Asp[1545] (Gly, Tyr, and Tyr, respectively, at the equivalent locations in $Na_v1.5$). To examine the role of these residues in the isoform specificity of μ-CTX, we created and studied the $Na_v1.4$ constructs E1521G/K1252Y and D1545Y. Both E1521G/K1252Y (IC_{50} = 53.6 ± 17.6 nM, n = 3) and D1545Y (IC_{50} = 54.7 ± 9.1 nM, n = 3) channels displayed $Na_v1.4$-like sensitivity to μ-CTX GIIIB (p > 0.05), indicating that these variants in the conventional pore are not responsible for isoform-specific μ-CTX block of $Na_v1.4$ and $Na_v1.5$ Na^+ channels.

DII S5-P Linker Plays a Role in Isoform-specific μ-CTX Block of $Na_v1.4$ and $Na_v1.5$ Na^+ Channels—The lack of effect observed with isoform-specific mutations in the conventional pore prompted us to examine other channel regions. Comparison of the primary sequences of $Na_v1.4$ and $Na_v1.5$ reveals substantial divergence in the DII S5-P linkers. Sequence alignment of the two isoforms, however, is ambiguous because the $Na_v1.5$ linker is shorter than that in $Na_v1.4$, and the remaining residues contain numerous conservative differences. Fig. 1*B* shows the two alignments that we used as a guide to create DII S5-P $Na_v1.4$ constructs (isoform-specific residues mutated are identified by *asterisks*). Fig. 1*C* summarizes the effects of these variant mutations on μ-CTX GIIIB block. All DII S5-P mutants except Δ723C/V724R/Δ725C/K726R expressed functional channels. Because the deletion of Cys[723] and Cys[725] did not yield measurable currents, we studied the roles of these residues by serine substitution (*i.e.* C723S and C725S, respectively) as inspired by the Cys → Ser difference at position 731. Indeed, the isoform-specific point mutations V724R (IC_{50} = 111.4 ± 14.4 nM, n = 5), C725S (IC_{50} = 2.5 ± 0.1 μM, n = 6), A728S (IC_{50} = 364.3 ± 24.3 nM, n = 4), D730S (IC_{50} = 5.5 ± 0.5 μM, n = 3), and C731S (IC_{50} = 1.6 ± 0.5 μM, n = 3) significantly reduced GIIIB block of μ1 by 4-, 86-, 12-, 185-, and 55-fold respectively, rendering the muscle isoform more "cardiac-like." Interestingly, N732D slightly improved toxin binding. To obtain further mechanistic insights, we also studied the mutations A728V and A728L (Fig. 2*A*). Of the mutations at the 728 position, A728L channels displayed the lowest sensitivity to GIIIB (IC_{50} = 1.4 ± 0.2 μM, n = 3) followed by A728V (IC_{50} = 1.1 ± 0.4 μM, n = 4), A728S, and WT $Na_v1.4$. Because leucine has the largest side chain (124 Å³), followed by valine (105 Å³), serine (73 Å³), and alanine (67Å³), these observations are consistent with the notion that side chain volume at position 728 influences toxin block and that μ-CTX binding is optimal when an alanine is present. For channel position 730, we neutralized the native cationic residue also by replacing it with an asparagine (*i.e.* D730N). Similar to D730S, D730N showed significantly reduced GIIIB block (IC_{50} = 3.0 ± 0.3 μM, n = 4, p < 0.05). Interestingly, although the charge-conserved mutation D730E (IC_{50} = 553.4 ± 77.9 nM, n = 4) improved toxin block compared with D730S and D730N channels, the charge-re-

versed mutation D730K (IC_{50} = 1.6 ± 0.2 μM, n = 3) did not worsen it compared with the charge-neutralized substitutions D730S and D730N, as might have been anticipated from a simple electrostatic effect. Instead, D730K channels were >2-fold more susceptible than either of the neutral counterparts. These results of Asp[730] mutations are summarized in Fig. 2*B*.

A DII S5-P $Na_v1.5$ Chimeric Construct Displayed Enhanced Sensitivity to μ-CTX—If the DII S5-P isoform-specific variants identified above are truly responsible for isoform-specific μ-CTX block of $Na_v1.4$, then conversion of the equivalent residues in $Na_v1.5$ to those in $Na_v1.4$ should enhance the sensitivity of the toxin-resistant heart channels. However, it should be pointed out that no single residue completely reproduced the cardiac sensitivity. The closest was D730S, whose "isoform specificity" is somewhat debatable because the sequence alignment in this region is ambiguous, as shown in Fig. 1*B*, and because of the seemingly important steric role of DII S5-P, as gauged by the mutations at position 728. We postulate that the spacing between these residues plays a role in high affinity toxin block of WT $Na_v1.4$. Therefore, we created a $Na_v1.5$ → $Na_v1.4$ (heart-to-muscle or H-to-M) chimera in which 10 consecutive DII S5-P residues from $Na_v1.4$ were spliced into the "homologous" region of $Na_v1.5$ (Fig. 3*A*). Although falling short of reproducing the high affinity μ-CTX block seen in $Na_v1.4$ ($Na_v1.4$ H-to-M IC_{50} = 4.2 ± 1.3 μM, n = 7), block by 5 μM μ-CTX GIIIB was enhanced significantly in the DII S5-P $Na_v1.5$ chimeric construct (60.7 ± 7.5%, n = 7) compared with the WT $Na_v1.5$ (31.2 ± 8.9%, n = 3; p < 0.05; Fig. 3*B*).

Different DII S5-P Variants Underlie Isoform-specific μ-CTX Block of $Na_v1.1$ and $Na_v1.4$—Although the amino acid differences between $Na_v1.4$ and $Na_v1.5$ at positions 724, 725, 728, 730, and 731 in the DII S5-P linker appear to modulate μ-CTX block prominently, these residues are absolutely conserved between $Na_v1.1$ and $Na_v1.4$ (Fig. 4*A*) and thus cannot explain their known difference in μ-CTX sensitivity (11, 12). Further sequence comparison of the DII S5-P linker of the muscle and brain isoforms reveals two other unique variants at positions 729 and 732: serine and asparagine in $Na_v1.4$ compared with threonine and lysine in $Na_v1.1$. To test their roles, we replaced the $Na_v1.4$ residues Ser[729] and Asn[732] with those in $Na_v1.1$ and studied their effects (Fig. 4, *B* and *C*). Consistent with the notion that the DII S5-P linker plays a prominent role in determining the isoform-specific μ-CTX response, the chimeric single mutations S729T (IC_{50} = 100.1 ± 22.4 nM, n = 3) and N732K (IC_{50} = 249.6 ± 100.7 nM, n = 8) rendered $Na_v1.4$ more "brain-like" by reducing their sensitivity. Similar to N732K, replacement of residue 732 with an arginine (N732R), which also places a positive charge at the same position but with a slightly larger side chain volume (148 Å³ *versus* 135 Å³ of lysine), also reduced GIIIB block (IC_{50} = 151.1 ± 25.8 nM, n = 3; Fig. 5). Combining S729T and N732K mutations (S729T/N732K) further decreased μ-CTX sensitivity (IC_{50} = 904.9 ± 286.0 nM, n = 4) to a level comparable with that of WT $Na_v1.1$ (IC_{50} = 2686.5 ± 138.8 nM, n = 6; Fig. 4, *B* and *C*), suggesting that the effects of these mutations were additive.

To confirm the isoform-specific role of residues 729 and 732, we next converted the analogous residues in $Na_v1.1$ simultaneously to those of $Na_v1.4$ (*i.e.* $Na_v1.1$-T925S/K928N). Indeed, this chimeric double mutation reproduced the high affinity μ-CTX GIIIB block observed with $Na_v1.4$ channels (IC_{50} = 52.8 ± 10.6 nM, n = 4; Fig. 4, *B* and *C*). Collectively, our data substantively bolster the notion that the DII S5-P linker is a determinant for isoform-specific μ-CTX block.

Differential Sensitivities to μ-CTX GIIIA and GIIIB—Even though μ-CTX GIIIA and GIIIB have nearly identical backbone structures and block WT $Na_v1.4$ with the same affinity, we
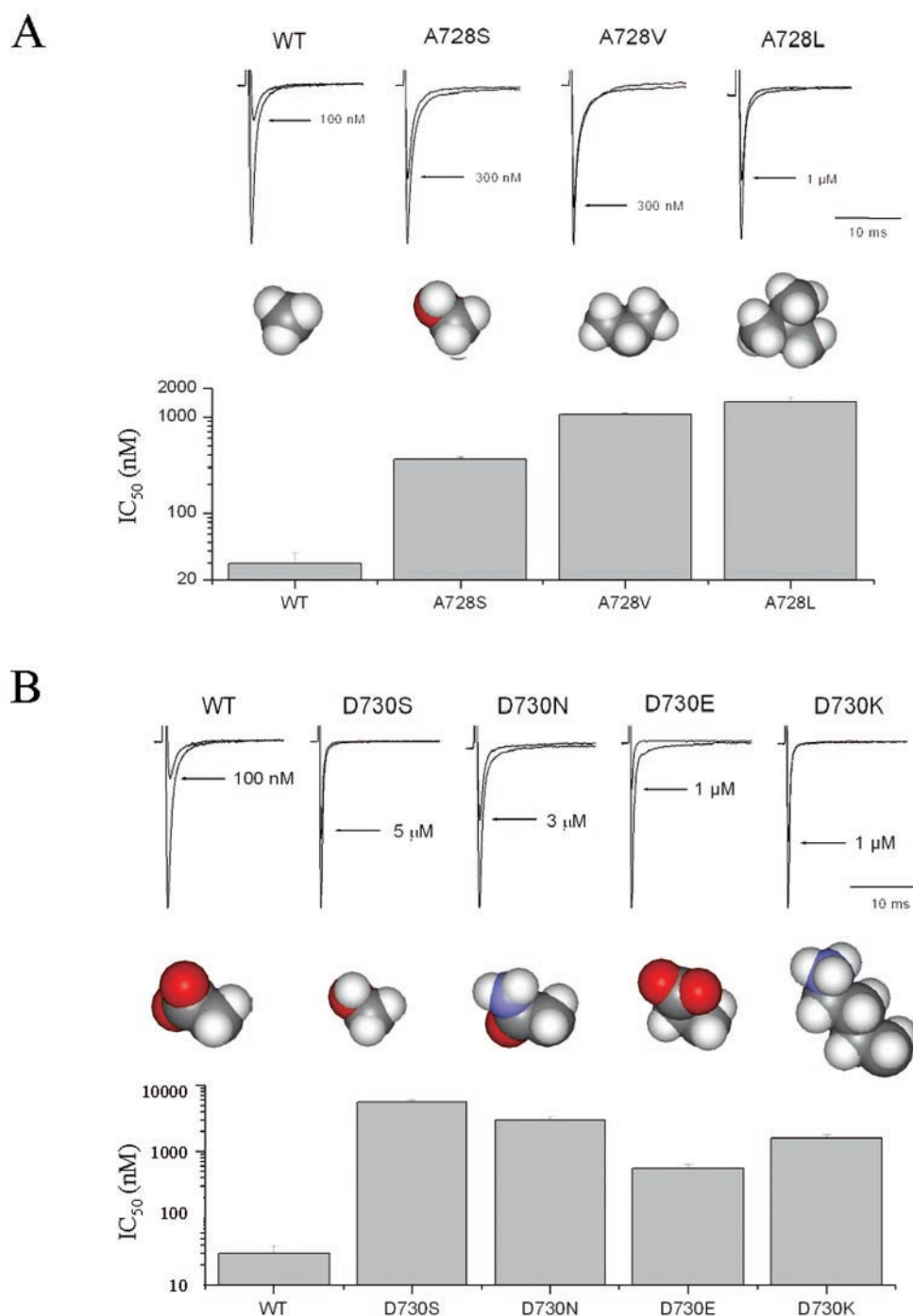
Molecular Basis of Isoform-specific μ-CTX Block

FIG. 2. **Effects of multiple substitutions at positions 728 and 730 on μ-CTX sensitivity.** *A*: *top*, representative current tracings through WT, A728S, A728V, and A728L Na$_v$1.4 channels with or without μ-CTX as indicated. *Middle*, amino acid substitutions into position 728. Side chains are shown without their backbone atoms in the CPK format. Hydrogen, *white*; oxygen, *red*; carbon, *gray*; nitrogen, *blue*. *Bottom*, *bar graphs* summarizing the IC$_{50}$ values of the same channels for block by μ-CTX. A728V channels were less sensitive than A728S but more sensitive than A728L. Data shown are the mean ± S.E. *B*: *top*, typical raw current traces of WT, D730S, D730N, D730E, and D730K Na$_v$1.4 channels with or without μ-CTX as indicated. *Middle*, amino acid side chains substituted into position 730. *Bottom*, IC$_{50}$ summary.

recently reported that the negatively charged DII P-S6 residues Asp[762] and Glu[765], when mutated to lysine, confer upon Na$_v$1.4 channels the unique ability to distinguish between these toxin forms (20, 31–33). Because the DII S5-P variants identified are also in DII (in particular, the Asp → Lys N732K variant is also a lysine substitution), we tested whether our DII S5-P variant channels possessed such discriminative ability so as to obtain insights into this obscure channel region. Fig. 5 shows that V724R, C725S, A728S, S729T, D730N, and C731S channels had equal susceptibilities to GIIIA and GIIIB ($p >$

0.05). In contrast, although ~10-fold less sensitive to block by GIIIB than WT Na$_v$1.4, both N732K and N732R channels displayed GIIIA sensitivity not different from WT Na$_v$1.4 ($p >$ 0.05). Therefore, these constructs could discriminate between GIIIA and GIIIB in a manner similar to the DII P-S6 lysine mutants. Likewise, WT Na$_v$1.1 could also discriminate between the two toxin forms (IC$_{50}$ for GIIIA = 290.6 ± 11.4 nM, n = 11). This discriminative ability of WT Na$_v$1.1, however, was lost in the B-to-M chimeric double mutant (IC$_{50}$ for GIIIA = 52.8 ± 10.6 nM, n = 6).
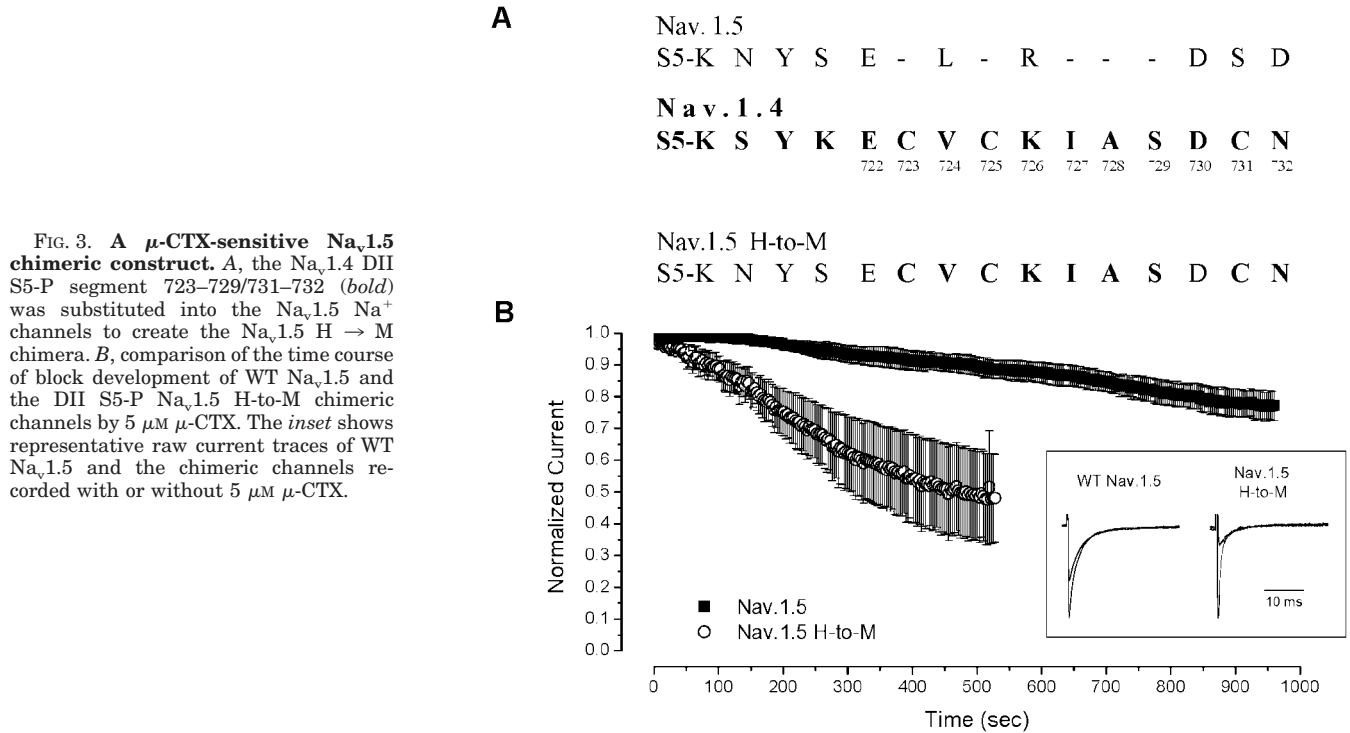
A

Nav. 1.5
S5-K N Y S E - L - R - - - D S D

Nav.1.4
S5-K S Y K E C V C K I A S D C N
722 723 724 725 726 727 728 729 730 731 732

Nav.1.5 H-to-M
S5-K N Y S E C V C K I A S D C N

FIG. 3. **A μ-CTX-sensitive Na$_v$1.5 chimeric construct.** *A*, the Na$_v$1.4 DII S5-P segment 723–729/731–732 (*bold*) was substituted into the Na$_v$1.5 Na$^+$ channels to create the Na$_v$1.5 H → M chimera. *B*, comparison of the time course of block development of WT Na$_v$1.5 and the DII S5-P Na$_v$1.5 H-to-M chimeric channels by 5 μM μ-CTX. The *inset* shows representative raw current traces of WT Na$_v$1.5 and the chimeric channels recorded with or without 5 μM μ-CTX.
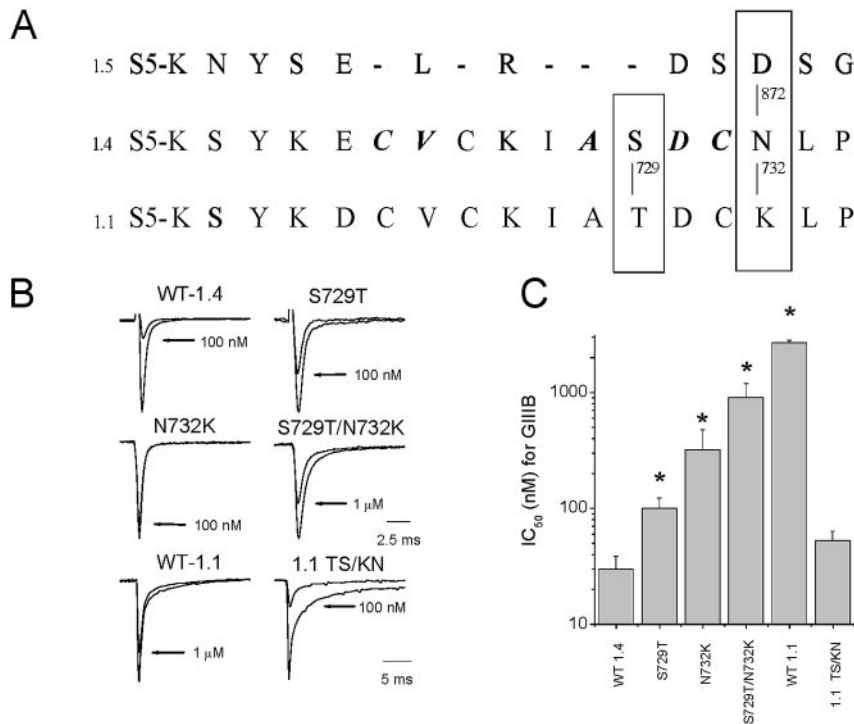
B

A

1.5 S5-K N Y S E - L - R - - - D S D S G

1.4 S5-K S Y K E *C V* C K I A *S D C* N L P
729 872 732

1.1 S5-K S Y K D C V C K I A T D C K L P

B

C

FIG. 4. **Effects of DII S5-P isoform variants between Na$_v$1.1 and Na$_v$1.4 on μ-CTX block.** *A*, comparison of the DII S5-P linkers of Na$_v$1.1 and Na$_v$1.4 Na$^+$ channels. The critical DII S5-P variants identified for Na$_v$1.4 and Na$_v$1.5 in Fig. 2 are absolutely conserved between Na$_v$1.1 and Na$_v$1.4. Sequence comparison of these isoforms reveals two other differences at Na$_v$1.4 positions 729 and 732. *B*, representative Na$^+$ currents through WT, S729T, N732K, and S729T/N732K Na$_v$1.4 channels and those through WT and T925S/K928N (*TS/KN*) Na$_v$1.1 channels recorded in the absence and presence of μ-CTX GIIIB. *C*, *bar graph* summarizing the IC$_{50}$ for μ-CTX GIIIB block of the same channels from *B*. The mutations S729T, N732K, and S729T/N732K rendered Na$_v$1.4 less sensitive to μ-CTX block, whereas the converse chimeric mutation T925S/K928N rendered Na$_v$1.1 more sensitive with an affinity similar to Na$_v$1.4. *, p < 0.05.

Effects of N732K/D762K/E765K on μ-CTX GIIIA and GIIIB Sensitivities—Reversing both the DII P-S6 negative charges at positions 762 and 765 by lysine substitution (D762K/E765K) results in an additional decrease in GIIIB (but not GIIIA) block compared with the individual single mutations alone, suggesting that both charges are required simultaneously for high affinity GIIIB block (10, 20). We next investigated whether a similar additive effect was observed when N732K from DII S5-P and the DII P-S6 mutations are combined. The triple mutation N732K/D762K/E765K rendered Na$_v$1.4 channels highly insensitive to μ-CTX GIIIB (IC$_{50}$ = 110 ± 25 μM; n = 4) but only modestly reduced GIIIA block (IC$_{50}$ = 182.4 ± 90.8 nM;

n = 3). Fig. 6 shows a typical toxin experiment performed with this channel construct. Application of 5 μM GIIIB to N732K/D762K/E765K channels produced no significant current blockade, and 10 μM GIIIB blocked I_{Na} only to 92.4 ± 4.5% of the control toxin-free level (*versus* ~87% block of D762K/E765K with 3 μM GIIIB; see Fig. 4 of Ref. 20). Thus, the effect of N732K on GIIIB block and those of the DII P-S6 mutations were largely additive. In contrast, application of 300 nM GIIIA to N732K/D762K/E765K mutant channels substantially reduced I_{Na} to 33.8 ± 10.6%. Therefore, N732K/D762K/E765K, as anticipated from the blocking phenotypes of the individual mutations, could also discriminate between GIIIA and GIIIB.

Molecular Basis of Isoform-specific μ-CTX Block

FIG. 5. **Differential sensitivities of Na⁺ channels to μ-CTX GIIIA and GIIIB.** Representative Na⁺ current tracings through N732K and WT Na$_v$1.1 channels measured in the absence and presence of GIIIA and GIIIB are shown as indicated (*top panel*). *Bar graphs* summarizing the IC$_{50}$ values of various Na$_v$1.4 and Na$_v$1.1 channels for block by μ-CTX GIIIA and GIIIB are shown in the *bottom panel*. N732K, N732R, and WT Na$_v$1.1 channels displayed differential sensitivities to GIIIA and GIIIB (*, $p < 0.05$). All other DII S5-P Na$_v$1.4 variants as well as Na$_v$1.1-T925S/K928N (*TS/KN*) were equally insensitive to both GIIIA and GIIIB forms of μ-CTX.
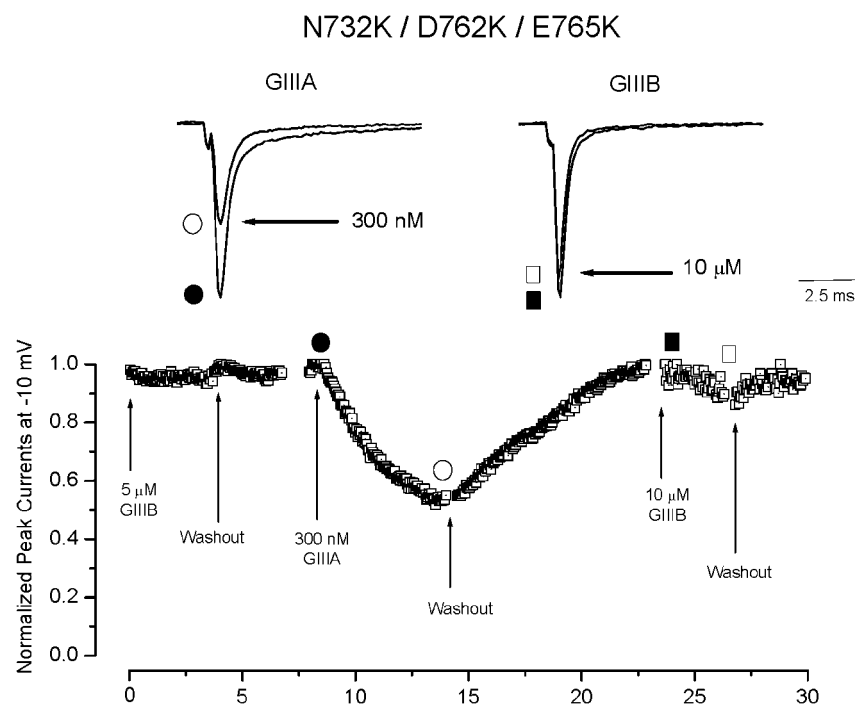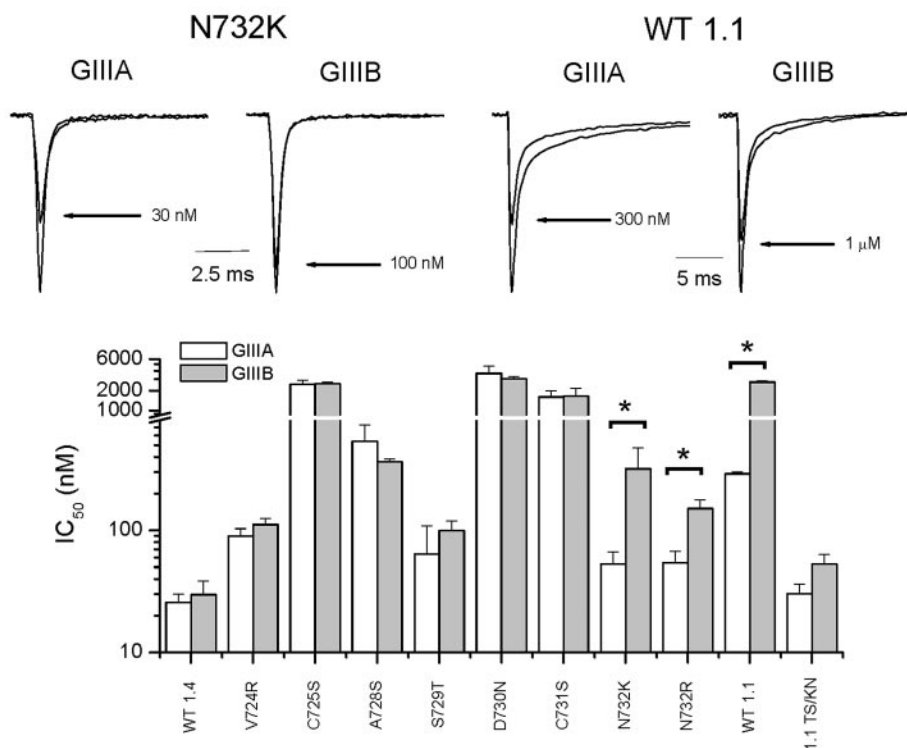

FIG. 6. **Effects of the triple mutation N732K/D762K/E765K on μ-CTX block.** *Top panel*, representative Na⁺ currents through N732K/D762K/E765K channels in the absence and presence of 300 nM μ-CTX GIIIA (*left*) and 10 μM GIIIB (*right*) as indicated. As anticipated from the individual single mutations, N732K/D762K/E765K was insensitive to GIIIB but sensitive to GIIIA. The effect of combining the individual DII lysine mutations (N732K, D762K, and E765K) on GIIIB block was additive (*cf.* Refs. 10 and 20). *Bottom panel*, a typical experiment demonstrating the time course of the development of onset and offset of GIIIA and GIIIB block of N732K/D762K/E765K during toxin washin and washout as indicated. Normalized peak sodium currents elicited by depolarization to −10 mV from a holding potential of −100 mV were plotted *versus* time in minutes.

DISCUSSION

Ion channels with similar ionic selectivity may differ significantly in other properties related to the pore, such as drug and toxin sensitivity. As mentioned, skeletal muscle Na⁺ channels exhibit sensitivity to block by μ-CTX which is 2 orders of magnitude greater than their cardiac and brain counterparts. Although previous studies have identified critical pore residues for high affinity μ-CTX block (8–10, 22–24, 34), these residues are well conserved among different channel isoforms and therefore cannot explain their vastly different toxin sensitivities. To look for the molecular components responsible for such isoform-specific differences, we switched our focus to the DII S5-P

linker, a highly variable region lying N-terminal to the highly conserved conventional pore formed by the P loop and the P-S6 linker (11, 24). Although previous studies of Na⁺ channels have mostly focused on the conserved pore region, the S5-P linkers of other ion channels have been reported to regulate properties such as toxin sensitivity, gating, and permeation (28, 35, 36). In this study, we provided evidence that isoform-specific variants in the DII S5-P linker of Na⁺ channels play a prominent role in shaping their distinctive isoform-specific sensitivity to μ-CTX block. Although not explored here, changes of gating properties (particularly of current decay) were also observed with some of these DII S5-P variant mutants (*e.g.* A728S and H-to-M chime-

FIG. 7. **A schematic representation of isoform-specific μ-CTX interactions with Na$_v$1.1 (*left*), 1.4 (*middle*), and 1.5 (*right*) channels.** When the Na$_v$1.4 determinants in the DII S5-P linker (*red*) are disrupted (in Na$_v$1.1) or absent (in Na$_v$1.5), the μ-CTX receptor in the pore becomes distorted or concealed such that optimal high affinity μ-CTX binding cannot occur despite the presence of all other receptor constituents in the P loops (*purple*) in these isoforms. The four Na$^+$ channel domains are arranged in a *clockwise* configuration (19). The binding orientation of μ-CTX to Na$_v$1.4 is based on previously identified toxin-channel interactions (19, 20, 21). The positions of Na$_v$1.4 residues 729 and 732 (925 and 928 of Na$_v$1.1) are only approximate.
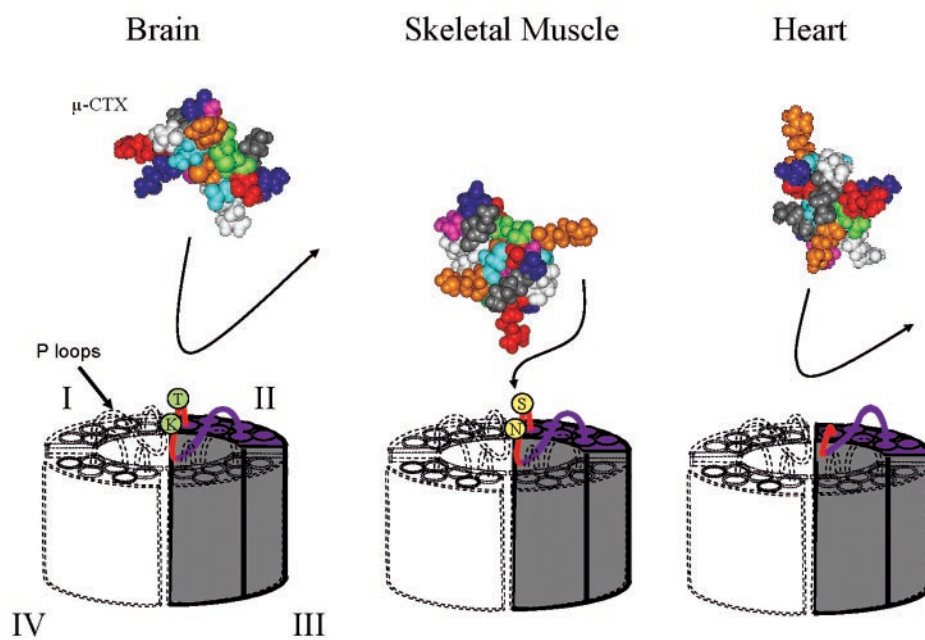
ra). Taken collectively, our present results further highlight the functional importance of this extracellular linker.

Different Molecular Bases Underlie Isoform-specific μ-CTX Block of Na$_v$1.4, Na$_v$1.5, and Na$_v$1.1 Na$^+$ Channels—Interestingly, all of the sequence variants that alter μ-CTX block of Na$_v$1.4 and Na$_v$1.5 (*i.e.* Val[724], Cys[725], Ala[728], Asp[730], Cys[731]) are absolutely conserved between Na$_v$1.1 and Na$_v$1.4 channels. However, we found that the variants between Na$_v$1.1 and Na$_v$1.4 within the same linker at positions 729 and 732 also modulate μ-CTX block. These results are consistent with previous chimeric studies demonstrating that DII plays the most important role in determining isoform-specific μ-CTX block (15). Taken collectively, it is clear that amino acid differences in the DII S5-P linkers of Na$_v$1.1, Na$_v$1.4, and Na$_v$1.5 channels figure prominently in their distinctive isoform-specific μ-CTX sensitivities. This notion is bolstered by the enhanced μ-CTX sensitivity observed with the toxin-resistant Na$_v$1.1 and Na$_v$1.5 channels when the converse DII S5-P chimeric mutations were introduced. However, although the B-to-M Na$_v$1.1 double mutant reproduced the high affinity blocking phenotype of Na$_v$1.4, the H-to-M Na$_v$1.5 chimeric construct only modestly enhanced μ-CTX block of the cardiac channel. These observations suggest that the basis for isoform-specific μ-CTX block is more complex in the cardiac channel and is likely to involve as yet other unidentified structural determinants. Other channel regions (*e.g.* DI (15) and its S5-P linker in particular) are likely to be involved in modulating the isoform specificity of Na$_v$1.5. On the other hand, the weak gain-of-function phenotype may simply reflect the exacting nature of such experiments, in which one of many subtle structural features may suffice to undermine high affinity block. Nonetheless, it is obvious that the toxicological profiles of Na$_v$1.1, Na$_v$1.4, and Na$_v$1.5 Na$^+$ channels have different molecular bases, but all appear to involve the same channel region (*i.e.* the DII S5-P linker).

Discrimination between μ-CTX GIIIA and GIIIB—The isoform variant N732K is unique compared with other DII S5-P determinants because it enabled Na$_v$1.4 channels to distinguish between GIIIA and GIIIB (see Ref. 37). The importance of residue 732 in determining the ability of Na$^+$ channels to discriminate between the two toxin isoforms is illustrated further by our finding that WT Na$_v$1.1 but not Na$_v$1.1 T925S/K928N channels were blocked differentially by GIIIA and

GIIIB. Collectively, our present results further exemplify the principle of "latent specificity," in which the ability of a receptor to recognize homologous ligands can be rendered highly specific (or abolished) by engineering the amino acid backbone even in the absence of innate specificity (20). In fact, the ~170-fold difference in GIIIA and GIIIB sensitivities observed with the triple mutant N732K/D762K/E765K was by far the largest among those that we have reported (*i.e.* D762K, E765K, D762K/E765K, D762Q/E765Q) to possess this unique discriminative ability (20). Our results may have pragmatic implications for future biosensor design.

We have shown previously that combining the individual DII P-S6 charge-reversed mutations D762K and E765K (*i.e.* D762K/E765K) further destabilizes GIIIB block compared with the corresponding single mutations alone. However, the additional reduction is only ~4-fold, a relatively small change compared with the ~200-fold decrease observed with the individual single substitutions (10, 20). These observations highlight the plausibility that the DII P-S6 residues may have common and/or preferential interacting toxin partners (19, 20). In contrast, we found that the ~5-fold reduction in GIIIB block observed with the triple mutant N732K/D762K/E765K relative to D762K/E765K channels was highly comparable with the 10-fold decrease in toxin sensitivity caused by the single mutation N732K alone compared with WT Na$_v$1.4, suggesting that the effects of N732K and the DII P-S6 mutations on GIIIB block were largely independent and additive. Cummins *et al.* (37) suggest that the DII S5-S6 loop may have a topology that allows residues 732, 762, and 765 to align along the same axis and interact simultaneously with Arg[14] of GIIIB, the charge-change toxin variant that underlies the differential binding of GIIIA and GIIIB to the DII P-S6 mutants (20, 37). Our data further suggest that Lys[732] is likely to influence toxin binding via mechanisms independent of the DII P-S6 residues. Given the improvement and reduction of block observed with N732D and N732K (and N732R) channels, respectively, it is possible that residue 732 interacts directly with the toxin molecule and/or with other native charged side chains of the channel. Further experiments using toxin derivatives and mutant cycle analysis may provide additional insights and are currently under way. Regardless of the underlying mechanism, it is clear that the variant at position 732 plays a critical role in deter-

mining the isoform-specific differences in μ-CTX binding between Na$_v$1.1 and Na$_v$1.4 but not Na$_v$1.5 channels and the ability of channels to distinguish between the GIIIA and GIIIB forms of μ-CTX.

Structural and Pharmacological Implications—Recently, French and colleagues (38) proposed that μ-CTX inhibits Na$^+$ currents in at least two ways. First, the physical bulk of μ-CTX (molecular weight ~2,600) sterically blocks the channel vestibule. Second, basic residues protruding from different faces of the toxin molecule reduce the effective capture volume from which ions enter the pore. Most importantly, the charge of Arg[13] appears to neutralize the effects of native acidic pore residues (such as Glu[758]) that serve to increase the effective Na$^+$ concentration at the external pore mouth. Clearly, high affinity μ-CTX binding to the pore requires optimal positioning of residues that contribute to the toxin receptor.

The S5-P linker, N-terminal to the "descending" limb of the P loop (SS1), is not thought to line the pore or to interact with the toxin directly (9, 14). This notion is supported by several lines of evidence. Asp[730] is unexposed when probed by cysteine substitution and sulfhydryl-modifying agents (14). Furthermore, there is no observable molecular interaction (≪1 kcal/mol when probed by thermodynamic mutant cycle analysis) between the isoform-specific sequence variants V724R, A728S, D730S (data not shown) and the Arg[13]-Gln[14]-Lys[16]-Arg[19] helical receptor-binding domain of μ-CTX which is known to interact prominently with the DII pore-lining segment of Na$_v$1.4 (19, 20, 39). Based on these lines of reasoning, we hypothesize that the DII S5-P determinants identified here may act as steric spacers that allosterically modulate or control the access of other nearby pore-lining residues (such as Glu[758], Asp[762], and Glu[765]) that interact or are in direct contact with the surface-blocking μ-CTX. This steric theory is consistent with the dependence of toxin sensitivity on the side chain volume at position 728 and the lack of obvious electrostatic effects with the isoform variants at position 730. During the preparation of this manuscript, Cummins *et al.* (37) reported that GIIIB binding is correlated inversely to the size of residue 729 (IC$_{50}$ of S729L > S729T > S729A ≈ WT Na$_v$1.4) (37). Our findings that residue 732 modulates μ-CTX block and that the toxin sensitivity follows N732D ≈ WT Na$_v$1.4 > N732R > N732K is also consistent with their results for a similar sensitivity sequence of WT Na$_v$1.4 ≈ N732E ≈ N732Q > N732K (37). Taken collectively, we propose a general model for isoform-specific μ-CTX-channel interactions. When the DII S5-P determinants are absent (or disrupted), the channel receptor in WT Na$_v$1.5 (or Na$_v$1.1) becomes concealed so that high affinity μ-CTX binding cannot occur despite the presence of all other receptor constituents (such as Glu[403], Glu[758], Asp[762], Glu[765], Asp[1241], and Asp[1532] (8–10, 23) in the conserved Na$^+$ channel pore (Fig. 7). This "concealed receptor" theory is similar to the "guarded receptor" theory (40) except that access to the receptor is static rather than gated. It can be generalized to explain other isoform-specific protein-ligand interactions. Although an active site or a ligand receptor may be well conserved among different isoforms of the same protein class, isoform-specific properties may differ markedly because of surrounding regions that do not otherwise participate directly in the biological activity in question. Because these "scaffolds" are usually more variable among different isoforms, they may represent unique sites for drug targeting whereby a relatively nonselective drug moiety

can be delivered to the nearby conserved active site with imposed specificity as a result of the increased local effective concentration around the active site caused by its binding to the targeted scaffolds (41).

REFERENCES

1. Cruz, L. J., Kupryszewski, G., LeCheminant, G. W., Gray, W. R., Olivera, B. M., and Rivier, J. (1989) *Biochemistry* **28,** 3437–3442
2. Cruz, L. J., Gray, W. R., Olivera, B. M., Zeikus, R. D., Kerr, L., Yoshikami, D., and Moczydlowski, E. (1985) *J. Biol. Chem.* **260,** 9280–9288
3. Gray, W. R., Rivier, J. E., Galyean, R., Cruz, L. J., and Olivera, B. M. (1983) *J. Biol. Chem.* **258,** 12247–12251
4. Olivera, B. M., Rivier, J., Clark, C., Ramilo, C. A., Corpuz, G. P., Abogadie, F. C., Mena, E. E., Woodward, S. R., Hillyard, D. R., and Cruz, L. J. (1990) *Science* **249,** 257–263
5. Nakamura, H., Kobayashi, J., Ohizumi, Y., and Hirata, Y. (1983) *Experientia* (*Basel*) **39,** 590–591
6. Moczydlowski, E., Olivera, B. M., Gray, W. R., and Strichartz, G. R. (1986) *Proc. Natl. Acad. Sci. U. S. A.* **83,** 5321–5325
7. Yanagawa, Y., Abe, T., and Satake, M. (1986) *Neurosci. Lett.* **64,** 7–12
8. Dudley, S. C., Jr., Todt, H., Lipkind, G., and Fozzard, H. A. (1995) *Biophys. J.* **69,** 1657–1665
9. Li, R. A., Tsushima, R. G., Kallen, R. G., and Backx, P. H. (1997) *Biophys. J.* **73,** 1874–1884
10. Li, R. A., Ennis, I. L., Velez, P., Tomaselli, G. F., and Marbán, E. (2000) *J. Biol. Chem.* **275,** 27551–27558
11. Fozzard, H. A., and Hanck, D. A. (1996) *Physiol. Rev.* **76,** 887–926
12. Moczydlowski, E., Uehara, A., Guo, X., and Heiny, J. (1986) *Ann. N. Y. Acad. Sci.* **479,** 269–292
13. Marbán, E., Yamagishi, T., and Tomaselli, G. F. (1998) *J. Physiol.* **508,** 647–657
14. Chahine, M., Sirois, J., Marcotte, P., Chen, L., and Kallen, R. G. (1998) *Biophys. J.* **75,** 236–246
15. Chen, L. Q., Chahine, M., Kallen, R. G., Barchi, R. L., and Horn, R. (1992) *FEBS Lett.* **309,** 253–257
16. Backx, P. H., Yue, D. T., Lawrence, J. H., Marbán, E., and Tomaselli, G. F. (1992) *Science* **257,** 248–251
17. Heinemann, S. H., Terlau, H., and Imoto, K. (1992) *Pflügers Arch.* **422,** 90–92
18. Satin, J., Kyle, J. W., Chen, M., Bell, P., Cribbs, L. L., Fozzard, H. A., and Rogart, R. B. (1992) *Science* **256,** 1202–1205
19. Li, R. A., Ennis, I. I., French, R. J., Dudley, S. C., Jr., Tomaselli, G. F., and Marbán, E. (2001) *J. Biol. Chem.* **276,** 11072–11077
20. Li, R. A., Ennis, I. L., Tomaselli, G. F., French, R. J., and Marbán, E. (2001) *Biochemistry* **40,** 6002–6008
21. Li, R. A., Sato, K., Kodama, K., Kohno, T., Xue, T., Tomaselli, G. F., and Marbán, E. (2002) *FEBS Lett.* **511,** 159–164
22. Dudley, S. C., Jr., Chang, N., Hall, J., Lipkind, G., Fozzard, H. A., and French, R. J. (2000) *J. Gen. Physiol.* **116,** 679–690
23. Chang, N. S., French, R. J., Lipkind, G. M., Fozzard, H. A., and Dudley, S., Jr. (1998) *Biochemistry* **37,** 4407–4419
24. Li, R. A., Velez, P., Chiamvimonvat, N., Tomaselli, G. F., and Marbán, E. (1999) *J. Gen. Physiol.* **115,** 81–92
25. Li, R. A., Ennis, I. I., Tomaselli, G. F., and Marbán, E. (2001) *Circulation* **104,** II–309 (abstr.)
26. Johns, D. C., Nuss, H. B., and Marbán, E. (1997) *J. Biol. Chem.* **272,** 31598–31603
27. Smith, R. D., and Goldin, A. L. (1998) *J. Neurosci.* **18,** 811–820
28. Xue, T., and Li, R. A. (2002) *J. Biol. Chem.* **277,** 46233–46242
29. Hamill, O. P., Marty, A., Neher, E., Sakmann, B., and Sigworth, F. J. (1981) *Pflügers Arch.* **391,** 85–100
30. Gellens, M. E., George, A. L., Jr., Chen, L. Q., Chahine, M., Horn, R., Barchi, R. L., and Kallen, R. G. (1992) *Proc. Natl. Acad. Sci. U. S. A.* **89,** 554–558
31. Hill, J. M., Alewood, P. F., and Craik, D. J. (1996) *Biochemistry* **35,** 8824–8835
32. Wakamatsu, K., Kohda, D., Hatanaka, H., Lancelin, J. M., Ishida, Y., Oya, M., Nakamura, H., Inagaki, F., and Sato, K. (1992) *Biochemistry* **31,** 12577–12584
33. Lancelin, J. M., Kohda, D., Tate, S., Yanagawa, Y., Abe, T., Satake, M., and Inagaki, F. (1991) *Biochemistry* **30,** 6908–6916
34. Li, Y., and Moczydlowski, E. (1991) *J. Biol. Chem.* **266,** 15481–15487
35. Dun, W., Jiang, M., and Tseng, G. N. (1999) *Pflügers Arch.* **439,** 141–149
36. Pardo-Lopez, L., Zhang, M., Liu, J., Jiang, M., Possani, L. D., and Tseng, G. N. (2002) *J. Biol. Chem.* **277,** 16403–16411
37. Cummins, T. R., Aglieco, F., and Dib-Hajj, S. D. (2002) *Mol. Pharmacol.* **61,** 1192–1201
38. Hui, K., Lipkind, G., Fozzard, H. A., and French, R. J. (2002) *J. Gen. Physiol.* **119,** 45–54
39. Sato, K., Ishida, Y., Wakamatsu, K., Kato, R., Honda, H., Ohizumi, Y., Nakamura, H., Ohya, M., Lancelin, J. M., and Kohda, D. (1991) *J. Biol. Chem.* **266,** 16989–16991
40. Starmer, C. F., Grant, A. O., and Strauss, H. C. (1984) *Biophys. J.* **46,** 15–27
41. Li, R. A., Tsushima, R. G., Himmeldirk, K., Dime, D. S., and Backx, P. H. (1999) *Circ. Res.* **85,** 88–98

Molecular Basis of Isoform-specific μ-Conotoxin Block of Cardiac, Skeletal Muscle, and Brain Na $^{+}$ Channels

Ronald A. Li, Irene L. Ennis, Tian Xue, Hai M. Nguyen, Gordon F. Tomaselli, Alan L. Goldin and Eduardo Marbán

Access the most updated version of this article at doi: 10.1074/jbc.M210882200

Alerts:
- When this article is cited
- When a correction for this article is posted

Click here to choose from all of JBC's e-mail alerts

This article cites 40 references, 20 of which can be accessed free at
http://www.jbc.org/content/278/10/8717.full.html#ref-list-1